Biocompatible Silk Printed Optical Waveguides

By *Sara T. Parker, Peter Domachuk, Jason Amsden, Jason Bressner, Jennifer A. Lewis, David L. Kaplan,* and *Fiorenzo G. Omenetto**

The necessity for optical interfaces in biomedical applications is driving increasing demand for the development of biocompatible photonic components. Biophotonic components are essential for applications including sensors,[1,2] imaging,[3–6] bio-microelectromechanical systems (MEMS) devices,[7] and therapeutics.[8] Silk fibroin in film form has been recently identified as a suitable biopolymer for the development of optical devices.[9,10] Biocompatible silk fibroin has promise as an optical biomaterial based on a number of important physical properties.[11] In particular, silks are the strongest and toughest natural fibers known, and regenerated silk fibroin from the *Bombyx mori* silkworm are easily formed into a variety of material formats such as hydrogels,[12] ultrathin and thick films,[13,14] controlled-release coatings,[15] 3D porous matrices,[16] and fibers with controllable diameters.[17] In addition to these structures, which are primarily for biomedical applications, silk fibroin has also been used to fabricate biocompatible and biodegradable microfluidic devices that can be used as biosensors or other BioMEMS devices.[18] Silk was found to be especially well suited for optical applications in film form with free standing materials of thickness between 20 and 100 μm, which are possible due to the strong β-sheet conformation that imparts the impressive mechanical properties. These films are ideal for optical devices, because they are mechanically robust, have very smooth surfaces with roughness <5 nm rms, are highly transparent (>95%) across the visible region of the spectrum, and can be patterned with transverse features of the order of a few tens of nanometers.[9,10] An additional feature of this silk fibroin protein is the feasibility of biochemical functionalization due to the benign processing used during film formation, which confers added versatility to these devices.

Although 2D and 3D optical elements based on silk films, including diffractive patterns, holograms, lenses, and optical gratings, have been demonstrated,[9,10] other optical components remain unexplored. Optical waveguides are of specific interest because of their ability to manipulate and transport light in a controlled manner. In many biomedical applications, these functional elements must interface directly with living cells, requiring the waveguide material to be biocompatible. For a biophotonic implantable device, it may also be required that the components be biodegradable. Hence, the use of a biocompatible and biodegradable polymer to guide light would open new opportunities for biologically based modulation and sensing, with potential for biomedical utility as well as environmental compatibility.[11,19]

Simple polymeric planar and channel waveguides are usually produced through complicated microfabrication, lithography, or lamination techniques.[20] These processes involve the use of harsh chemicals, salts, UV exposure, high temperature, or high pressure, all of which can be detrimental to biological components. For the fabrication of optical waveguides from biological molecules, a more benign approach is needed. Direct ink writing is a simple, flexible, and inexpensive technique that does not require harsh processing steps. During direct-write assembly, a computer-controlled three-axis translation stage precisely moves a syringe barrel that houses a viscous ink, which is extruded from a fine deposition nozzle under an applied pressure. The inks are designed to flow readily through the nozzle without clogging, yet undergo rapid solidification upon exiting the nozzle to retain its filamentary shape. Using direct-write assembly, the fabrication of simple and complex 3D structures has been demonstrated with a variety of materials, including polymeric,[21] sol–gel,[22] and colloidal inks.[23] Recently, we reported a new method for direct writing of 3D silk structures for tissue engineering from an aqueous solution of regenerated *B. mori* silk fibroin.[16] This approach can be readily extended to fabricate silk fibers into programmable patterns for optical applications, such as waveguides.

In this communication, we report on a technique to generate silk optical waveguides through direct ink writing. The silk fibroin ink consists of an aqueous solution of 28–30 wt% silk that is processed under mild ambient conditions. The printed silk waveguides retain their rodlike morphology by crystallizing in a methanol-rich, coagulation reservoir. Both straight and wavy silk fibers were patterned, and found to easily guide light from a He:Ne laser source with a wavelength of 633 nm. The optical loss measurements were comparable to those observed for thin silk films, proving that printed silk waveguides may find potential application in a variety of optical devices. A common laser dye, Rhodamine 6G, is added to representative silk waveguides as a gain medium to further demonstrate the flexibility of this approach. Our ability to print silk fibroin waveguides offers a new route for creating biophotonic elements that are both

[*] Prof. F. G. Omenetto, P. Domachuk, J. Amsden, J. Bressner
Department of Biomedical Engineering
and Department of Physics
Tufts University, 4 Colby Street
Medford, MA 02155 (USA)
E-mail: fiorenzo.omenetto@tufts.edu
S. T. Parker, Prof. J. A. Lewis
Department of Materials Science and Engineering
and Frederick Seitz Materials Research Laboratory
University of Illinois at Urbana-Champaign
1304 West Green Street, Urbana, IL 61801 (USA)
Prof. D. L. Kaplan
Department of Biomedical Engineering
and Department of Chemical Engineering
Tufts University, 4 Colby Street
Medford, MA 02155 (USA)

DOI: 10.1002/adma.200801580

biocompatible and biodegradable and can be readily doped or functionalized with a number of biologically active molecules.[9]

A schematic of the direct-write assembly approach for patterning silk optical waveguides is shown in Figure 1. Using a computer-controlled x–y–z positioning stage, an aqueous silk fibroin solution regenerated from *B. mori* silk cocoons is extruded through a 5 μm glass deposition nozzle into a methanol-rich reservoir in a programmed pattern. As previously shown,[16] the methanol-rich reservoir induces a structural transition in the silk fibroin ink, which transforms from an amorphous random coil conformation to stiff β-sheets that promote solidification of the extruded waveguides into the desired shape. The silk waveguides are printed on borosilicate glass slides in both straight and wavy configurations that can extend as long as several centimeters. The borosilicate glass substrates were found to have an index of refraction n of 1.52, slightly lower than that of silk, which was measured to be $n = 1.54$ (at 633 nm).[9,10] The higher refractive index of the silk fibroin is necessary to allow for light confinement in a silk waveguide at the substrate interface. Light confinement on the remaining sides of the silk waveguides is ensured by the air/silk interface. Notably, the refractive index of silk also exceeds that of water ($n \sim 1.33$), indicating that the silk waveguides would also fulfill requirements for guiding within a water-based biological environment.

To confine the emitted light within the silk during propagation, not only does the waveguide material need to present a higher index of refraction compared to that of the surrounding environment, but it must also have a suitable morphology. In order to realize a good waveguide, the transverse dimensions of the printed line must be as uniform as possible, while the walls of the waveguide must remain smooth and free of defects to minimize surface scattering and excessive losses. Figure 2a and b shows a top view of the straight and curved silk waveguides along with a cross-sectional view (Fig. 2c) of the printed silk filament. The dimensions of the waveguide cross-section are approximately 5 μm × 5 μm, in good agreement with the 5 μm nozzle size. The highly concentrated (28–30 wt%) silk fibroin ink helps to minimize directional shrinkage during drying. There is some deviation from a perfectly circular cross-section, because the ink wets and partially spreads on the substrate during the printing

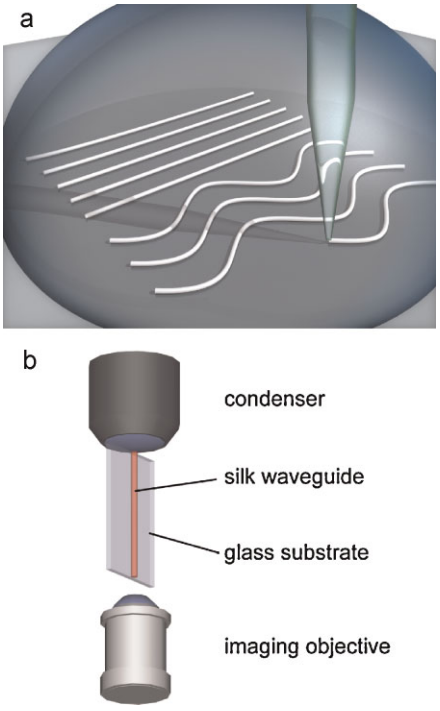

Figure 1. a) Schematic of direct-write assembly of silk waveguides in both straight and curvy patterns, in which a concentrated silk fibroin ink is extruded through a micronozzle into a methanol-rich coagulation reservoir. b) Schematic of the setup used to image and analyze the transverse face of the silk waveguides. The position of the optical condenser is adjustable for optimal coupling of light inside the silk waveguide.

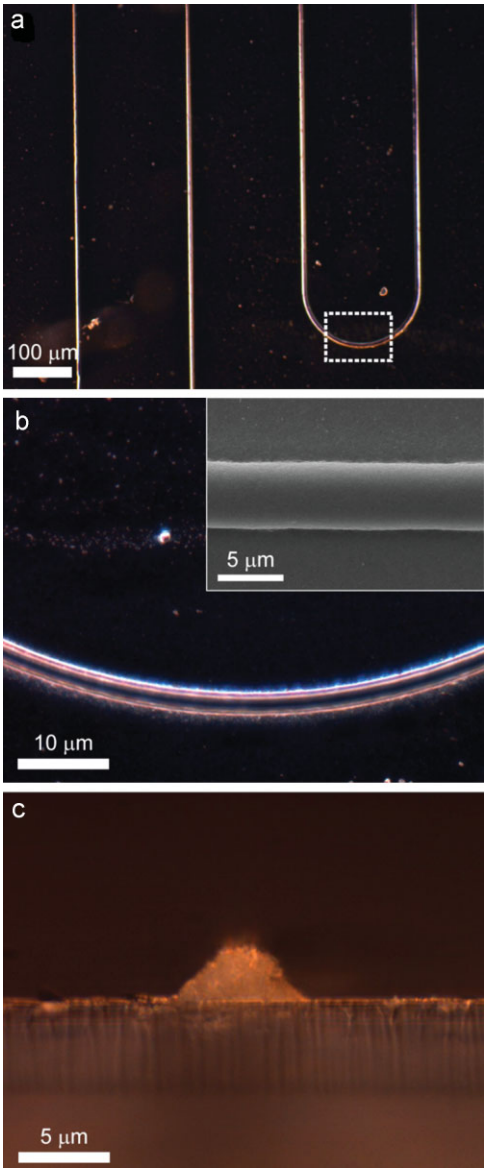

Figure 2. Optical images of a) printed silk waveguide, b) higher-magnification view of the curved feature highlighted by the dashed box in a), and c) cross-sectional view of the printed silk waveguide after cleavage to expose a clean interface for light coupling. The inset in b) depicts an SEM image of the surface morphology of a printed silk waveguide.

process before β-sheet crystallization occurs. This phenomenon yields printed silk features that possess a slightly trapezoidal crystallized shape. However, this shape provides a larger interface between the waveguide and substrate, improving adhesion. The transverse dimensions are consistent throughout the length of the waveguide, and no discontinuities are observed. Quantitative analysis of the images indicates a measured variation on the transverse dimension of less than 1% for both the straight and curved waveguides (Fig. 2a). The importance of the silk-ink quality is critical in this respect, as we have previously reported for silk-hydrogel formation.[24] A magnified scanning electron microscopy (SEM) image of the silk waveguide surface is shown in the inset of Figure 2b. The surface morphology is very smooth, and displays neither defects nor porosity, which helps to prevent scattering during light propagation. The consistent transverse dimensions, lack of discontinuities, and smoothness of the silk waveguides all contribute to their facile ability to guide light.

The optical quality of the printed silk features was analyzed by propagating light in the waveguides described above. Coupling light into the silk waveguides poses a challenge, because the printing technique does not generate an optically accessible fiber end. To remedy this, the substrates were etched with a diamond scribe and snapped apart, thereby exposing a smooth surface as the stiff silk waveguides fractured at the crack plane. Using this method, a transverse surface on the silk waveguide can be obtained that is suitable for optical coupling. Images of 633 nm He:Ne laser-light propagating through 1 cm portions of both straight and wavy silk waveguides are presented in Figure 3a and b. It is clear from the images that the light is indeed coupled into a single waveguide, since only one waveguide is illuminated in an array of printed silk fibers. Its wavy nature renders it apparent that the coupled light is propagating through the silk waveguide and not just in a straight line. By adjusting the position of the condenser, it was possible to optimize coupling of the illuminator light inside the silk waveguide and observe that the cleaved end lights up when guiding is achieved. This is also shown in Figure 3c, in which the cross-section of a silk waveguide with guided light is presented. This image contrasts greatly with Figure 2c, which shows the cross-section of a silk waveguide in the absence of light propagation.

Both straight and curved silk features guided light, thus loss measurements were performed to measure the quality of the guiding. The measured losses were $0.25\,dB \cdot cm^{-1}$ and $0.81\,dB \cdot cm^{-1}$ for the straight and curved waveguides, respectively. For comparison, the losses obtained by propagating light in 30 μm thick silk fibroin films yielded values between 0.25 and $0.75\,dB \cdot cm^{-1}$. The consistency of the values is a good indicator of the quality of the printed silk features, which compares favorably to the "optical-grade" silk material in film form previously reported.[10]

The simplicity of this method coupled with the ease of functionalization offered by the aqueous silk solution[10] allows for additional degrees of freedom when printing waveguides. By doping the silk-based ink with appropriate species, optically activated silk-fibroin-based waveguides can be readily manufactured. To demonstrate this, we printed a silk waveguide that was doped with rhodamine 6G, a known laser dye that was incorporated into the silk-fibroin solution prior to printing. The straight doped waveguides are characterized similarly to their

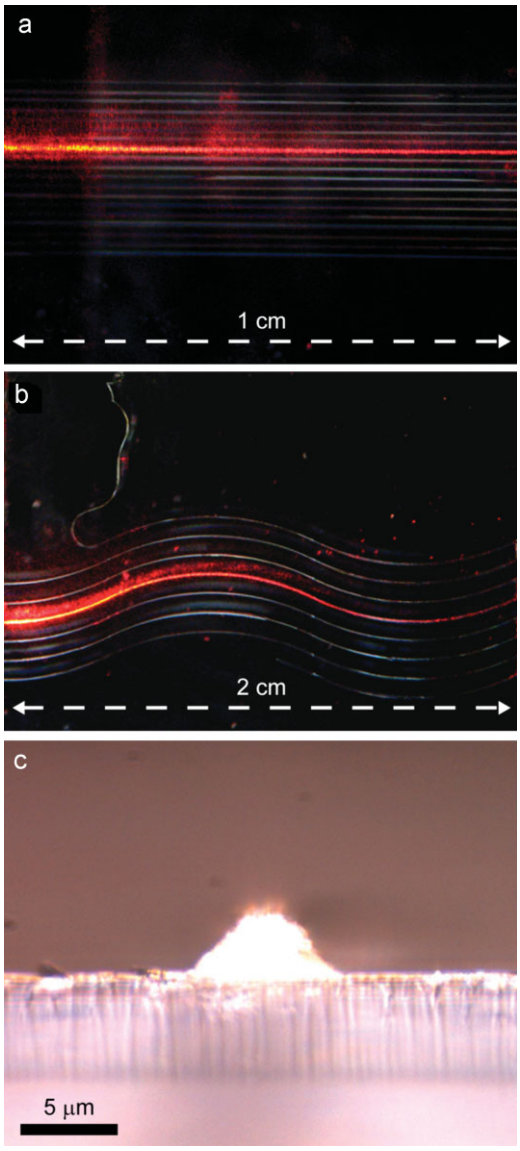

Figure 3. Optical images of a) straight and b) wavy silk waveguides guiding light from a He:Ne laser source. c) Transverse image of the output face of a silk waveguide when light is guided through the optical fiber.

undoped counterparts, and evaluated for uniformity and loss. In this case, 532 nm laser light is coupled into the doped-silk waveguides to match the absorption spectrum of the rhodamine dye. As light is propagated into the waveguide, a strong fluorescent emission centered at 555 nm is detected. The waveguide glows uniformly yellow from the propagating green light, which can be easily seen when imaged through a green filter (Fig. 4). The fluorescent spectrum is measured along the waveguide and is found to be constant throughout its length. The losses in this 1 cm segment of waveguide are very low, and are estimated to be $<0.1\,dB \cdot cm^{-1}$, which represents the best result to date in these structures.

In conclusion, we report a new method for fabricating microscale biopolymer waveguides with controlled structure and composition. Through direct-write assembly of a highly concentrated aqueous solution of pure silk-fibroin protein, we

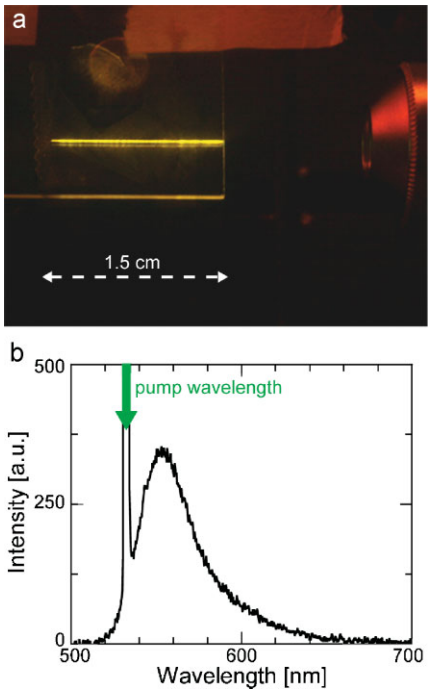

Figure 4. a) Fluorescence image of 1.5 cm rhodamine 6G-doped silk waveguide stimulated with green 532 nm laser light. The image is filtered at this wavelength, allowing the yellow emission from the doped waveguide to be clearly visible. b) Plot of intensity as a function of wavelength from the doped waveguide in a), which illustrates the 532 nm wavelength of the pump laser and the corresponding fluorescence spectrum centered at 555 nm resulting from the emission of the rhodamine 6G-doped silk waveguide.

patterned both pure and doped silk waveguides in the form of straight and wavy architectures. The optical properties of these waveguides further establish the efficacy of silk fibroin as a high-quality biocompatible optical material. Direct-write assembly of silk optical waveguides can be readily extended to a variety of geometries, serving as a starting point for the development of biophotonic chips based on traditional slab waveguide designs. Our approach provides a facile avenue for creating biocompatible, biodegradable, and biologically functionalized optics and optical interfaces, as well as designing new biophotonic sensing devices based on the interaction with light. Furthermore, the ability to biochemically functionalize or incorporate dopants into the silk-fibroin ink allows for unconventional photoactivation of the waveguides, which is not easily achieved in glass or other inorganic waveguides. Together, these advances provide a new enabling platform for the emerging field of biophotonics. Further, recent reports on the favorable mechanical properties of methanol-processed silk films [11] and of direct-write, methanol-processed silk fibers [16] renders this approach suitable for manufacturing free-standing silk optical fibers expanding the application space of these devices.

Experimental

Silk-Ink Preparation: Inks composed of 28–30 wt% aqueous silk-fibroin solution were prepared by concentrating 8 wt% regenerated silk solution prepared as described previously[15,19]. In brief, cocoons of *B. mori* silkworm silk (Tajima Shoji Co., Ltd., Yokohama, Japan) were boiled for 30 min in an aqueous solution of 0.02 M Na_2CO_3, and then rinsed thoroughly with distilled water to extract the glue-like sericin proteins. The extracted fibroin was dissolved in 9.3 M LiBr solution at 60 °C for 4 h, yielding a 20 wt% aqueous solution. This solution was dialyzed against distilled water using Slide-a-Lyzer dialysis cassettes (MWCO 3500, Pierce Biotechnology, Rockford, IL) at room temperature for three days to remove the salt. The dialysate was centrifuged twice, each at −5 to 10 °C for 20 min, to remove impurities and aggregates. The solution obtained from this process was approximately 8 wt%. This silk-fibroin aqueous solution (8 wt%, 9 mL) was then dialyzed against a 15 wt% poly(ethylene glycol) (PEG) (8000 g mol^{-1}, Sigma–Aldrich Corporation, St. Louis, MO) solution at room temperature using Slide-a-Lyzer dialysis cassettes (MWCO 3500)[12]. The volume ratio of PEG solution to silk fibroin solution was 40:1. After approximately 14 h, the concentrated silk fibroin solution (28–30 wt%) was slowly removed by a syringe to avoid excessive shearing. All solutions were stored at 4 °C before use and concentrated silk inks were used within five days to minimize gelation.

Silk-Waveguide Fabrication: Silk waveguides were formed with micrometer-sized features using a three-axis micropositioning stage (ABL9000, Aerotech Inc., Pittsburgh, PA) controlled by customized software (3D Inks, Stillwater, OK). The concentrated silk-fibroin solution was housed in a syringe (barrel diameter = 4.6 mm, EFD Inc., East Providence, RI) that was mounted on the *x*–*y*–*z* stage. The silk-fibroin ink was extruded through a 5 μm tapered microcapillary nozzle that was pulled from a borosilicate glass tube (1.0 mm outer diameter and 0.58 mm inner diameter) using a P-2000 Laser Based Micropipette Puller (Sutter Instrument, Novato, CA) onto a stationary glass substrate. The silk ink was extruded under an applied pressure (800 Ultra dispensing system, EFD Inc.) of 20–70 kPa at a constant deposition speed of 2 mm s^{-1}. The ink was deposited into a coagulation reservoir (~200 μL) consisting of a methanol/(methanol + water) ratio of 0.86. As the ink exited the nozzle, the continuous rodlike filament formed retained its shape after rapid coagulation in the deposition reservoir. All structures were dried at ~22 °C and less than 35% relative humidity.

Silk waveguides of arbitrary geometry can be patterned by our approach. For these experiments, straight and wavy lines were printed on glass substrates to investigate the optical quality of the printed silk features and their ability to guide light. We note that more-complex 2D and 3D geometries can be obtained with this method.[16]

Waveguide Characterization: The structures of the printed silk waveguides were analyzed using optical microscopy (Olympus IX-71, Tokyo, Japan) and SEM (S-4700 Scanning Electron Microscope, Hitachi Ltd., Tokyo, Japan). Prior to SEM imaging, samples were coated with gold/palladium for 30–60 s (Emitech K575 Sputter Coater, Emitech Ltd., Ashford Kent, UK).

The index of refraction of the patterned silk features was characterized using a waveguide instrument (Metricon Co., Pennington, NJ), and found to be $n = 1.54$. The refractive index of the glass substrate was also measured and found to be $n = 1.52$.

To create clean silk-fiber interfaces for light to easily couple into, the silk waveguides were cleaved after printing, crystallization, and drying, by scoring the glass substrate with a diamond blade and snapping the glass. The silk waveguide-patterned glass substrate was cleaved on both ends and then mounted vertically on an inverted microscope. The exposed fiber interface was illuminated by a dark-field condenser with variable numerical aperture (0.8–0.92). To estimate the optical loss along the waveguide, we measured the intensity variation of the scattered light directly above the waveguide along the direction of light propagation. The waveguides were mounted on a mechanical *x*–*y*–*z* flexure stage and He:Ne laser light ($\lambda = 633$ nm) was focused into the endface of both the straight and curved devices. For comparison, the losses obtained by propagating light in 30 μm thick, 3 cm × 3 cm silk films was also measured using a waveguide instrument (Metricon Co., Pennington, NJ).

Rhodamine 6G-Doped Silk Waveguides: Doped silk waveguides were fabricated by adding 4.0 mg rhodamine 6G (Sigma–Aldrich Corporation) to 10 g of the dilute 8 wt% silk-fibroin solution and gently stirring for ~2 h.

Notably, the rhodamine 6G did not fully dissolve into the silk solution. Any undissolved solids were removed prior to dialysis. The silk ink was then prepared, printed, and characterized in the same manner as described above for the undoped waveguides. Additionally, the doped waveguides were stimulated using 200 mW of CW laser light from a doubled Nd:YVO_4 solid state laser (Verdi V-10, Coherent Inc., Santa Clara, CA) operating at a wavelength of 532 nm. Optical images were obtained using a digital camera (Canon Rebel XTi, Canon Inc., Tokyo, Japan) fitted with a green glass filter (OD $>$ 6 at 532 nm) to eliminate the green scatter from the pump laser. The emission spectrum was measured by placing the tip of a fiber bundle in close proximity to the printed waveguide and coupling it into a portable spectrometer (USB2000, Ocean Optics, Dunedin, FL).

Acknowledgements

This work was partly funded by a National Science Foundation Graduate Research Fellowship (STP), the Defense Advanced Research Projects Agency (FGO), the Air Force Office of Scientific Research (DLK), and by the US Department of Energy under grant DE-FG02-07ER46471 (STP, JAL).

Received: June 9, 2008
Revised: February 5, 2009
Published online: April 8, 2009

[1] J. I. Peterson, G. G. Vurek, *Science* **1984**, *224*, 123.
[2] V. S. Y. Lin, K. Motesharei, K. P. S. Dancil, M. J. Sailor, M. R. Ghadiri, *Science* **1997**, *278*, 840.
[3] C. H. Contag, B. D. Ross, *J. Magn. Reson. Imaging* **2002**, *16*, 378.
[4] J. G. Fujimoto, *Nat. Biotechnol.* **2003**, *21*, 1361.
[5] J. G. Fujimoto, C. Pitris, S. A. Boppart, M. E. Brezinski, *Neoplasia* **2000**, *2*, 9.
[6] V. Ntziachristos, J. Ripoll, L. H. V. Wang, R. Weissleder, *Nat. Biotechnol.* **2005**, *23*, 313.
[7] A. C. R. Grayson, R. S. Shawgo, A. M. Johnson, N. T. Flynn, Y. W. Li, M. J. Cima, R. Langer, *Proc. IEEE* **2004**, *92*, 6.
[8] J. L. West, N. J. Halas, *Annu. Rev. Biomed. Eng.* **2003**, *5*, 285.
[9] B. D. Lawrence, M. Cronin-Golomb, I. Georgakoudi, D. L. Kaplan, F. G. Omenetto, *Biomacromolecules* **2008**, *9*, 1214.
[10] H. Perry, L. Dal Negro, A. Gopinat, D. L. Kaplan, F. G. Omenetto, *Adv. Mater.* **2008**, *20*, 3070.
[11] G. H. Altman, F. Diaz, C. Jakuba, T. Calabro, R. L. Horan, J. S. Chen, H. Lu, J. Richmond, D. L. Kaplan, *Biomaterials* **2003**, *24*, 401.
[12] U. J. Kim, J. Y. Park, C. M. Li, H. J. Jin, R. Valluzzi, D. L. Kaplan, *Biomacromolecules* **2004**, *5*, 786.
[13] C. Y. Jiang, X. Y. Wang, R. Gunawidjaja, Y. H. Lin, M. K. Gupta, D. L. Kaplan, R. R. Naik, V. V. Tsukruk, *Adv. Funct. Mater.* **2007**, *17*, 2229.
[14] X. Y. Wang, H. J. Kim, P. Xu, A. Matsumoto, D. L. Kaplan, *Langmuir* **2005**, *21*, 11335.
[15] X. Y. Wang, X. Hu, A. Daley, O. Rabotyagova, P. Cebe, D. L. Kaplan, *J. Control. Release* **2007**, *121*, 190.
[16] S. Ghosh, S. T. Parker, X. Wang, D. L. Kaplan, J. A. Lewis, *Adv. Funct. Mater.* **2008**, *18*, 1.
[17] H. J. Jin, S. V. Fridrikh, G. C. Rutledge, D. L. Kaplan, *Biomacromolecules* **2002**, *3*, 1233.
[18] C. J. Bettinger, K. M. Cyr, A. Matsumoto, R. Langer, J. T. Borenstein, D. L. Kaplan, *Adv. Mater.* **2007**, *19*, 2847.
[19] S. Hofmann, H. Hagenmuller, A. M. Koch, R. Muller, G. Vunjak-Novakovic, D. L. Kaplan, H. P. Merkle, L. Meinel, *Biomaterials* **2007**, *28*, 1152.
[20] H. Ma, A. K. Y. Jen, L. R. Dalton, *Adv. Mater.* **2002**, *14*, 1339.
[21] G. M. Gratson, M. J. Xu, J. A. Lewis, *Nature* **2004**, *428*, 386.
[22] E. B. Duoss, M. Twardowski, J. A. Lewis, *Adv. Mater.* **2007**, *19*, 3485.
[23] J. E. Smay, G. M. Gratson, R. F. Shepherd, J. Cesarano, J. A. Lewis, *Adv. Mater.* **2002**, *14*, 1279.
[24] A. Matsumoto, J. Chen, A. L. Collette, U. J. Kim, G. H. Altman, P. Cebe, D. L. Kaplan, *J. Phys. Chem. B* **2006**, *110*, 21630.